

# Vortex Rings and Mutual Drag in Trapped Bose-Einstein Condensates

B. Jackson, J. F. McCann\*, and C. S. Adams

*Dept. of Physics, Rochester Building, University of Durham, South Road, Durham, DH1 3LE, UK.*

(February 25, 2018)

We study the drag on an object moving through a trapped Bose-Einstein condensate, and show that finite compressibility leads to a mutual drag, which is subsequently suppressed by the formation of a vortex ring.

PACS numbers: 03.75.Fi, 67.40.Vs, 67.57.De

The appearance of vortices in quantum fluids has important consequences for many physical systems [1,2]. In particular, there appears to be a direct link between vortex formation and the breakdown of superfluidity in liquid helium [3]. However, a quantitative comparison between theory and experiment is impeded by the complexity of this many-body system.

The recent observation of Bose-Einstein Condensation (BEC) in trapped alkali gases [4], on the other hand, has yielded an ideal testing ground for many-body theories. Dilute condensates can now be produced at temperatures far below the BEC transition, allowing an accurate description by the Gross-Pitaevskii (GP) equation. By studying this equation, insight can be gained into the relationship between vortex formation and drag in superfluid systems. For homogeneous fluid flow past an obstacle, numerical studies show that below a critical velocity the fluid exerts no net force on the object [5], whereas above this velocity vortices are nucleated, leading to a pressure imbalance which creates drag [6].

The picture is less clear, however, in trapped Bose gases, which are inhomogeneous and of finite size. Simulations have shown that dragging an object, created by a far-detuned laser beam, through an inhomogeneous condensate produces compression waves and a series of vortex pairs [7]. The formation of these structures will influence the dynamics of the condensates and the drag on the object. An attractive system for studying drag is the multi-component condensate [8], where the magnetic sensitivity of the different hyperfine states allows the fluid components to be intermingled or spatially separated. In this paper, we simulate actively dragging a small condensate, the ‘object’, through a larger, less tightly confined condensate, the ‘fluid’. We find that a mutual drag arises due to deformation of the compressible object, which is relieved by the formation of vortex rings in the fluid. The time dependence of the mutual drag provides a signature of ring formation. This process is analogous to ring nucleation by moving ions in superfluid  $^4\text{He}$  [9], albeit on a different scale.

The numerical methods follow closely those employed in our previous work [7,10]. The coupled GP equations

for the condensate wavefunctions,  $\psi_i(\mathbf{r}, t)$ , in the  $x - y$  plane can be written as:

$$i\partial_t\psi_i = [-\nabla^2 + V_i + C(\alpha_i|\psi_i|^2 + |\psi_j|^2) - \mu_i]\psi_i, \quad (1)$$

where  $i, j = 1, 2$  ( $i \neq j$ ),  $\mu_i$  are the chemical potentials at equilibrium,  $V_i$  are the trap potentials,  $\alpha_i$  are the ratios of the scattering lengths, and  $C$  is the nonlinear coefficient [11]. We have performed 2D, cylindrically-symmetric 3D, and full Cartesian 3D simulations [12].

To demonstrate that coupled GP equations give an accurate description of the formation of structure in the condensate, we begin by modelling an experiment on component separation [13]. We assume that a condensate initially in state  $|1\rangle$  with trapping potential  $V_1 = (x^2 + \epsilon^2 y^2)/4$ , is subject to an interaction which transfers 50% of the population into state  $|2\rangle$ , which experiences a displaced potential  $V_2 = (x^2 + \epsilon^2(y - y_0)^2)/4$ , where  $y_0$  is the offset [14]. The displaced potential causes the two components to separate and subsequently oscillate at large amplitudes. Nonlinear mixing [15] leads to excitation of high-order modes, which appear as structure in the density profiles [13]. Fig. 1(a) displays a density cross-section at  $t = 8.52$  (corresponding to 65 ms). However, in the experiment, most of the structure had disappeared by this time. This disparity may be due to Landau damping at finite temperatures, where condensate excitations are absorbed by the thermal cloud. To simulate this effect, we propagate the GP equations (1) in complex time  $t \rightarrow (1 + i\Lambda)\tilde{t}$  [16]. Components with an energy,  $E$ , decay exponentially at a rate proportional to the damping constant,  $\Lambda < 0$  [17], and to  $E - \mu_i$ , in agreement with theory for the collisionless low-energy regime [18]. Higher frequency excitations are preferentially damped, reducing the density variation within the condensate (Fig. 1(b)).

Fig. 2 shows the center-of-mass position of the two condensates ( $Y_i = \iint y|\psi_i|^2 dx dy$ ) as a function of time. Population of high-energy excitations results in damping of the dipole mode, in agreement with previous work [19]. However, this mechanism alone is insufficient to explain the observed experimental damping. Propagation in complex time results in further damping, but at a relatively slow rate. We also investigate the effect of an offset in the  $x$ -direction, which may arise as a consequence of the experimental geometry [20]. In this case, mixing between the fast ( $y$ ) and slow ( $x$ ) vibrational modes [21] could be more significant than finite temperature effects in explaining the observed damping (see Fig. 2), though it is likely that a combination of these mechanisms is

responsible.

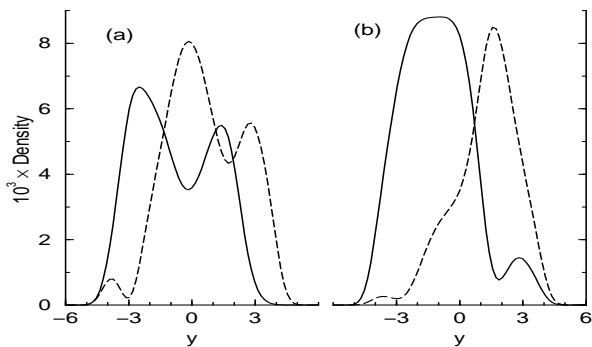


FIG. 1. Cross-sections through 2D density profiles,  $|\psi_1|^2$  (dashed) and  $|\psi_2|^2$  (solid), at  $x = 0$  and  $t = 8.52$ , showing results of (a) undamped, and (b) damped ( $\Lambda = -0.025$ ) propagation.

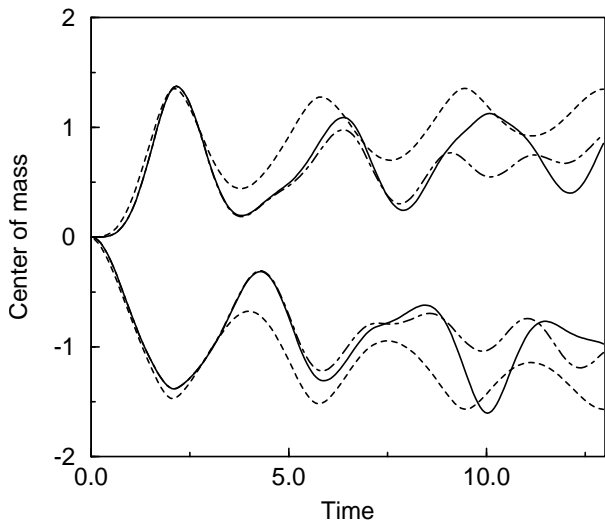


FIG. 2. Center-of-mass oscillations,  $Y_i(t)$ , in  $|1\rangle$  (top) and  $|2\rangle$ , for undamped (solid) and damped  $\Lambda = -0.025$  (dashed) propagation. The dot-dashed lines show the effect on undamped propagation of an additional offset,  $x_0 = 0.240$ , where decay of the oscillations are more marked than even a large Landau damping.

As is apparent in Fig. 2, over short timescales ( $t < 2$ ) thermal damping is negligible and the undamped GP equations provide a reliable model. We now turn to the situation where one condensate flows through the other, in direct analogy with an object moving through a fluid. This may be realized experimentally by using a magnetic trap to confine atoms in state  $|2\rangle$ , whilst an optical dipole trap, moving with relative velocity  $-v$ , loosely confines atoms in a magnetically insensitive level  $|1\rangle$ . We employ the coupled equations (1), with  $V_1 = (x^2 + y^2)/4$  and  $V_2 = V_1 + (x^2 + (y - vt)^2)$ , and  $\alpha_i = 1$ . The initial state is found using imaginary time propagation [22]. The repulsive mean field arising from the ‘object’ ( $|2\rangle$ ) creates

a local minimum in the center of the density profile of the ‘fluid’ ( $|1\rangle$ ) [23]. The depth of the minimum depends on the interaction strength  $C$ , and on the fraction of atoms in the fluid,  $f$ .

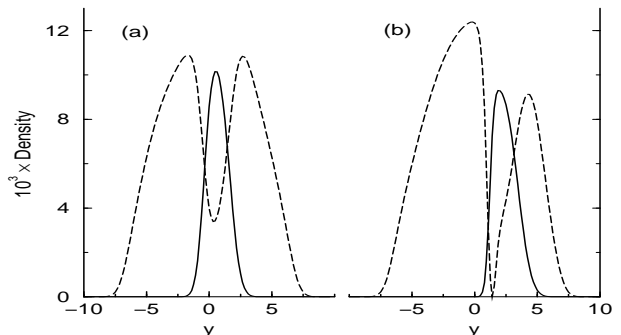


FIG. 3. Cross-sections through 2D density profiles at  $x = 0$ . Condensate  $|2\rangle$  (the ‘object’, solid line) moves through  $|1\rangle$  (the ‘background fluid’, dashed), due to displacement of trap potentials at constant velocity,  $v = 3$ ;  $C = 1050$ ,  $f = 0.95$  (where  $f$  is the fraction of atoms in  $|1\rangle$ ). Two time-frames are shown: (a)  $t = 0.75$ , where drag arises from a process analogous to phonon emission from the accelerating object, (b)  $t = 1.3$ , where deformation of the object and surrounding fluid leads to an additional drag.

Displacement of the object potential ( $V_2$ ) at  $t > 0$  induces motion of the object, which leads to the minimum in the background fluid becoming progressively deeper at a rate which increases with  $v$  (see Fig. 3). When the density minimum reaches zero, it evolves into a vortex ring. In addition, motion of the object creates a response in the fluid, implying a back-action, or drag, on the object. The drag may be studied through the center-of-mass acceleration, given by:

$$\ddot{\mathbf{R}}_i(t) = -2 \int_V |\psi_i(\mathbf{r}, t)|^2 \nabla \mu_i(\mathbf{r}, t) d^3 \mathbf{r}. \quad (2)$$

For steady flow of an homogeneous condensate without vorticity, the integral vanishes, implying superfluidity [24]. However, for a finite inhomogeneous system there is no steady state and a different criterion for superfluidity should be sought. There are four energy terms that contribute to the acceleration; however, the kinetic and self-interaction terms are found to be negligible, leaving only:

$$\ddot{Y}_{i,\text{trap}}(t) = -2 \iint |\psi_i|^2 \frac{\partial V_i}{\partial y} dx dy, \quad (3)$$

and,

$$\ddot{Y}_{i,\text{mut}}(t) = -2C \iint |\psi_i|^2 \frac{\partial}{\partial y} |\psi_j|^2 dx dy, \quad (4)$$

which correspond to the contributions from the trap potentials and the interaction between condensates, respectively.

The mutual acceleration (4) is particularly interesting in addressing the issue of drag. Fig. 4 shows the calculated mutual acceleration as a function of time. At later times ( $t > 2$ ) the condensates repel due to the inhomogeneity in the background fluid. For  $t < 2$  the acceleration is negative, implying an effective attraction, or equivalently a drag on the object.

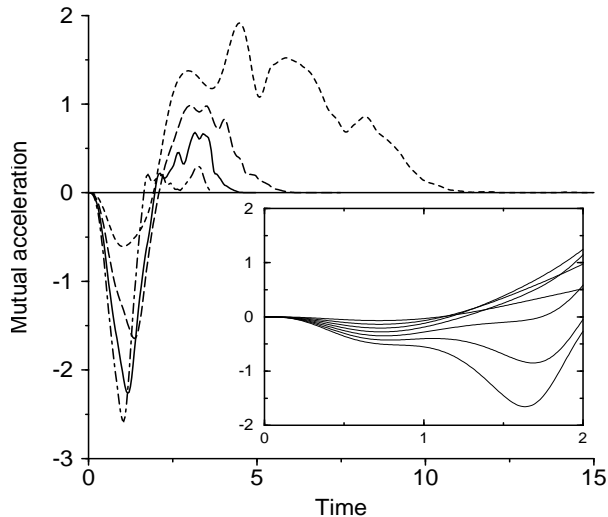


FIG. 4. Plot of  $\ddot{Y}_{2,\text{mut}}(t)$  for  $C = 600$ ,  $f = 0.83$ ;  $v = 1, 2, 3, 4$ . The ‘drag’ is evaluated from the minima of the curves, which increases in magnitude as the velocity rises. Inset shows a similar plot ( $C = 1050$ ,  $f = 0.95$ ) for  $v = 0.25$  to  $v = 1.75$  in steps of 0.25. At low  $v$  the local minima arise due to the finite response of the background fluid, [1]. At higher  $v$  an additional minimum appears at  $t > 1$  due to the compressibility of the object. The position of each minimum coincides with the moment of vortex formation.

For  $t < 1$  and low velocities, Fig. 4 (inset), the force results from the slow response of the fluid to the object acceleration. The object moves to the front of the potential well it creates in the mean field of the fluid, resulting in a restoring force which persists until the fluid can respond (Fig. 3(a)). The maximum attractive drag (i.e. the minima in Fig. 4) is plotted as a function of velocity in Fig. 5. This process, which is equivalent to phonon emission by an accelerating object, is responsible for the linear section of the drag curve.

For velocities near the speed of sound in the object,  $c_2 = \sqrt{2C|\psi_2|^2}$ , the object begins to deform, with the result that the overlap between the two fluids is reduced behind and enhanced in front (Fig. 3(b)). This increases the drag, producing the additional minima at  $t > 1$  in Fig. 4 (inset). Onset of this process is rapid with increasing velocity, giving rise to a sharp transition in the drag curve. This transition can be compared to that between superflow and normal flow in the homogeneous

system [5,6]. However, due to the finite size of the background fluid there is no steady flow condition, and drag is produced even at low velocities.

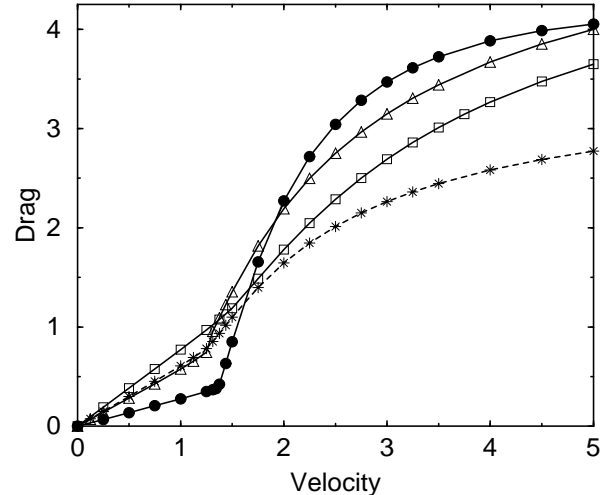


FIG. 5. Peak mutual attraction (drag) as a function of velocity. Curves are shown for: \*  $C = 600$ ,  $f = 0.83$ ;  $\Delta$   $C = 1100$ ,  $f = 0.91$ ;  $\square$   $C = 1200$ ,  $f = 0.83$ ;  $\bullet$   $C = 1050$ ,  $f = 0.95$ . The curves show linear dependence of drag at low velocities, and enhanced drag at high velocity due to the compressibility of the condensates. The magnitude of the additional drag is enhanced for highly compressible object condensates i.e. when  $1 - f$  is small, or when the mean-field interaction between condensates is large.

The drag force increases with time until the local minimum in the background fluid reaches zero (Fig. 3(b)), from which a vortex ring is formed. Subsequent expansion of the ring results in the condensate minimum being filled, thereby decreasing the pressure imbalance across the object. The object returns to a more symmetric shape, and the drag decays, as is apparent in Fig. 4. Hence, vortex formation in this context tends to limit or reduce the drag.

In summary, we simulate a scheme where one condensate is pulled through another, and identify mutual drag effects, and vortex ring creation which acts to suppress drag. Although vortex rings would be difficult to detect directly, we have shown that they produce a significant change in the mutual drag which could be observable.

Financial support for this work was provided by EPSRC. We are grateful to E. A. Cornell (JILA) for providing us with information on the experiment reported in [13].

\* New address: Dept. of Applied Mathematics, Queen’s

University, Belfast, BT7 1NN, UK.

- [1] D. R. Tilley and J. Tilley, *Superfluidity and Superconductivity* (IOP Publishing, Bristol, 1990).
- [2] T. W. B. Kibble, *J. Phys. A* **9**, 1387 (1976).
- [3] R. J. Donnelly, *Quantized Vortices in Helium II* (Cambridge University Press, Cambridge, 1991).
- [4] M. H. Anderson *et al.*, *Science* **269**, 198 (1995); K. B. Davis *et al.*, *Phys. Rev. Lett.* **75**, 3969 (1995); C. C. Bradley, C. A. Sackett, and R. G. Hulet, *Phys. Rev. Lett.* **78**, 985 (1997).
- [5] T. Frisch, Y. Pomeau, and S. Rica, *Phys. Rev. Lett.* **69**, 1644 (1992).
- [6] T. Winiecki, J. F. McCann, and C. S. Adams, preprint cond-mat/9812080.
- [7] B. Jackson, J. F. McCann, and C. S. Adams, *Phys. Rev. Lett.* **80**, 3903 (1998).
- [8] C. J. Myatt, E. A. Burt, R. W. Ghist, E. A. Cornell, and C. E. Wieman, *Phys. Rev. Lett.* **78**, 586 (1997).
- [9] G. W. Rayfield and F. Reif, *Phys. Rev.* **136**, 1194 (1964).
- [10] B. Jackson, J. F. McCann, and C. S. Adams, *J. Phys. B* **31**, 4489 (1998).
- [11] Throughout this paper, harmonic oscillator units (h.o.u.) are used, where for atoms of mass  $m$  trapped in a harmonic trap of frequency  $\omega$ , the units of length, time and energy are  $(\hbar/2m\omega)^{1/2}$ ,  $\omega^{-1}$  and  $\hbar\omega$  respectively. As a result of this scaling, the wavefunction is redefined so that the total density,  $|\psi_1|^2 + |\psi_2|^2$ , is normalised to unity, and  $C_{2D} = 8\pi N a_{12}$ , where  $N$  is the total number of atoms per unit length along the  $z$ -axis. We define  $\alpha_1 = a_1/a_{12}$  and  $\alpha_2 = a_2/a_{12}$ , where the scattering lengths between atoms in the same hyperfine level are denoted by  $a_1$  and  $a_2$ , while  $a_{12}$  represents scattering between hyperfine states.
- [12] We used a Fast Fourier Transform method, where a 2D wavefunction is typically discretized on a  $256 \times 256$  grid inside a  $40 \times 40$  box, while for 3D we employed a  $128 \times 128 \times 64$  grid. The time-step,  $\Delta t$ , must be small enough to ensure stability over sufficiently long propagation times;  $\Delta t = 5 \times 10^{-4}$  is adequate for most purposes.
- [13] D. S. Hall, M. R. Matthews, J. R. Ensher, C. E. Wieman, and E. A. Cornell, *Phys. Rev. Lett.* **81**, 1539 (1998).
- [14] Parameters in our simulations are chosen to reflect closely those in the experiment [13]. In particular,  $\epsilon = \sqrt{8}$ ,  $\omega = 2\pi \times 59/\sqrt{8}$ ,  $C = 3160$  and  $y_0 = 0.240$  h.o.u.  $\simeq 0.4 \mu\text{m}$ . Ratios of the scattering lengths are taken to be  $\alpha_1 = 1.03$  and  $\alpha_2 = 0.97$ , where  $a_{12} = 5.5$  nm.
- [15] P. A. Ruprecht *et al.*, *Phys. Rev. A* **51**, 4704 (1995); A. Smerzi and S. Fantoni, *Phys. Rev. Lett.* **78**, 3589 (1997); F. Dalfovo, C. Minniti, and L. P. Pitaevskii, *Phys. Rev. A* **56**, 4855 (1997); S. A. Morgan *et al.*, *Phys. Rev. A* **57**, 3818 (1998).
- [16] S. Choi, S. A. Morgan, and K. Burnett, *Phys. Rev. A* **57**, 4057 (1998).
- [17] To compare simulated lifetimes to physical results, we excite modes in a single condensate and propagate in complex time. Using this procedure, we estimate that a damping rate of  $\Lambda = -0.01$  corresponds to typical experimental values: D. S. Jin *et al.*, *Phys. Rev. Lett.* **77**, 420 (1996); D. S. Jin *et al.*, *Phys. Rev. Lett.* **78**, 764 (1997). However, we present results for  $\Lambda = -0.025$ , to clearly illustrate the physical effect of Landau damping.
- [18] L. P. Pitaevskii and S. Stringari, *Phys. Lett. A* **235**, 398 (1997); W. V. Liu, *Phys. Rev. Lett.* **79**, 4056 (1997); P. O. Fedichev, G. V. Shlyapnikov, and J. T. M. Walraven, *Phys. Rev. Lett.* **80**, 2269 (1998); S. Giorgini, *Phys. Rev. A* **57**, 2949 (1998).
- [19] A. Sinatra, P. O. Fedichev, Y. Castin, J. Dalibard, and G. V. Shlyapnikov, *Phys. Rev. Lett.* **82**, 251 (1999).
- [20] E. A. Cornell, personal communication.
- [21] Due to the anisotropy of the trap, the dipole mode corresponding to oscillations along the ‘slow’  $x$ -axis possesses a lower energy than along  $y$ . Displacement of the trap initially leads to oscillations along the ‘fast’ axis as previously; however, the broken symmetry now results in transitions that gradually populate the lower level.
- [22] B. D. Esry, C. H. Greene, J. P. Burke, and J. L. Bohn, *Phys. Rev. Lett.* **78**, 3594 (1997).
- [23] T.-L. Ho and V. B. Shenoy, *Phys. Rev. Lett.* **77**, 3276 (1996); H. Pu and N. P. Bigelow, *Phys. Rev. Lett.* **80**, 1130 (1998).
- [24] P. Nozières and D. Pines, *The Theory of Quantum Fluids* (Addison-Wesley, Redwood City, 1990), Vol. II.